THE JOURNAL OF BIOLOGICAL CHEMISTRY VOL. 285, NO. 22, pp. 16782–16788, May 28, 2010

Physical and Functional Interaction of Sequestosome 1 with Keap1 Regulates the Keap1-Nrf2 Cell Defense Pathway*[S]

Received for publication, December 18, 2009, and in revised form, March 27, 2010 Published, JBC Papers in Press, April 8, 2010, DOI 10.1074/jbc.M109.096545

Ian M. Copple[‡1], Adam Lister[‡1], Akua D. Obeng[‡], Neil R. Kitteringham[‡], Rosalind E. Jenkins[‡], Robert Layfield[§], Brian J. Foster[‡], Christopher E. Goldring[‡2], and B. Kevin Park[‡]

From the [‡]Medical Research Council Centre for Drug Safety Science, Department of Pharmacology and Therapeutics, the University of Liverpool, Sherrington Buildings, Ashton Street, Liverpool, L69 3GE and the [§]School of Biomedical Sciences, the University of Nottingham, Queens Medical Centre, Nottingham NG7 2UH, United Kingdom

Nrf2 regulates the expression of numerous cytoprotective genes in mammalian cells. The activity of Nrf2 is regulated by the Cul3 adaptor Keap1, yet little is known regarding mechanisms of regulation of Keap1 itself. Here, we have used immunopurification of Keap1 and mass spectrometry, in addition to immunoblotting, to identify sequestosome 1 (SQSTM1) as a cellular binding partner of Keap1. SQSTM1 serves as a scaffold in various signaling pathways and shuttles polyubiquitinated proteins to the proteasomal and lysosomal degradation machineries. Ectopic expression of SQSTM1 led to a decrease in the basal protein level of Keap1 in a panel of cells. Furthermore, RNA interference (RNAi) depletion of SQSTM1 resulted in an increase in the protein level of Keap1 and a concomitant decrease in the protein level of Nrf2 in the absence of changes in Keap1 or Nrf2 mRNA levels. The increased protein level of Keap1 in cells depleted of SQSTM1 by RNAi was linked to a decrease in its rate of degradation; the half-life of Keap1 was almost doubled by RNAi depletion of SQSTM1. The decreased level of Nrf2 in cells depleted of SQSTM1 by RNAi was associated with decreases in the mRNA levels, protein levels, and function of several Nrf2-regulated cell defense genes. SQSTM1 was dispensable for the induction of the Keap1-Nrf2 pathway, as Nrf2 activation by *tert*-butylhydroquinone or iodoacetamide was not affected by RNAi depletion of SQSTM1. These findings demonstrate a physical and functional interaction between Keap1 and SQSTM1 and reveal an additional layer of regulation in the Keap1-Nrf2 pathway.

Mammalian cells have evolved a multifaceted and highly regulated defense system to guard against the deleterious effects of chemical/oxidative stress. At the forefront of this system is the transcription factor Nrf2, which serves as a master regulator of the basal and inducible expression of an array of detoxification and antioxidant enzymes, through its action on the *cis*-acting antioxidant (or electrophile) response element regulatory motif (1). The important role of Nrf2 in directing this layer of cell defense has been emphasized in various studies that have demonstrated an increased susceptibility to xenobiotic-induced toxicity in Nrf2 knock-out animals (2–4).

In the absence of chemical/oxidative stress, the activity of Nrf2 is repressed by Keap1, a cysteine-rich protein that acts as a substrate adaptor for the cullin 3-dependent ubiquitination of Nrf2, thereby directing the transcription factor for proteasomal degradation (5–7). The "hinge and latch" model of Nrf2 regulation proposes that two distinct binding sites in Nrf2 facilitate the interaction with a Keap1 dimer (8). Binding to one molecule of Keap1 via the high affinity ^{79}ETGE^{82} motif within the Neh2 domain of Nrf2 provides the "hinge" through which the transcription factor can move in space relatively freely. Concomitant binding to a second Keap1 molecule via the lower affinity ^{29}DLG^{31} motif, also located within the Neh2 domain of Nrf2, provides the "latch" that tightly restricts Nrf2 to enable optimal positioning of target lysines for conjugation with ubiquitin (8).

Keap1 is able to "sense" chemical/oxidative stress at least partly via the modification of a subset of its numerous cysteine residues (9–12), although phosphorylation of Nrf2 may also play a role in determining the activity of this pathway (1). The modification of cysteine residues within Keap1 is postulated to cause a conformational change in the protein that disrupts the interaction between Keap1 and the low affinity ^{29}DLG^{31} motif within Nrf2, perturbing the ability of Keap1 to direct the ubiquitination and proteasomal degradation of the transcription factor (8). Hence, Keap1 becomes saturated with Nrf2 that cannot be efficiently degraded, and thus newly synthesized Nrf2 is free to accumulate within the nucleus and transactivate antioxidant (or electrophile) response element-driven cytoprotective genes (8).

Although Nrf2 is the only known substrate of Keap1, the latter has been reported to associate with several other proteins in mammalian cells (7, 13–17). In this study, we have used immunopurification of Keap1 and liquid chromatography coupled to electrospray ionization tandem mass spectrometry (LC-ESI-MS/MS)[3] to enable the identification of additional proteins that associate with Keap1 in the cellular milieu. As well as confirming the identity of some Keap1-interacting proteins already documented in the literature, this approach has identified the

* This work was supported by the Medical Research Council (UK), the Wellcome Trust, and the University of Liverpool.
⌘ *Author's Choice*—Final version full access.
[S] The on-line version of this article (available at http://www.jbc.org) contains supplemental Tables 1–4.
[1] Both authors contributed equally to this work.
[2] To whom correspondence should be addressed. Fax: 44(0)151-794-5540; E-mail: c.e.p.goldring@liv.ac.uk.

[3] The abbreviations used are: LC-ESI-MS/MS, liquid chromatography coupled to electrospray ionization tandem mass spectrometry; siRNA, short interfering RNA; RT, reverse transcription; GCLC, glutamate-cysteine ligase catalytic subunit; GAPDH, glyceraldehyde-3-phosphate dehydrogenase; IKKβ, inhibitor of κB kinase β; NF-κB, nuclear factor κB.

multifunctional protein sequestosome 1 (SQSTM1, also known as p62) (18) as a physiological binding partner of Keap1. Furthermore, evidence is provided to support the concept that SQSTM1 serves an important function in regulating the degradation of Keap1 and thus the integrity of the Keap1-Nrf2 pathway. As such, SQSTM1 contributes to the capacity of a cell to defend itself against chemical/oxidative stress.

EXPERIMENTAL PROCEDURES

Reagents—Unless noted, all reagents were from Sigma-Aldrich.

Cell Culture and Treatments—All cells were maintained at 37 °C in a 5% CO_2 atmosphere in Dulbecco's modified Eagle's medium (Cambrex, Nottingham, UK) supplemented with 584 mg/liter L-glutamine, 10% fetal bovine serum (Biowest, Nuaillé, France), 100 units/ml penicillin, and 100 μg/ml streptomycin. Nrf2 stabilization was induced by exposure of cells to 50 μM iodoacetamide or *tert*-butylhydroquinone for 1 h. To determine the half-life of Keap1, *de novo* protein synthesis was inhibited by exposure of cells to 35 μM cycloheximide for up to 16 h.

Expression and Immunopurification of Keap1-V5 and SQSTM1-FLAG—The full-length coding sequence of human Keap1 (Mammalian Gene Collection, IMAGE 1083678) was cloned without the stop codon and inserted into the TOPO cloning site of pcDNA3.1/V5-His-TOPO (Invitrogen). The human SQSTM1-FLAG/His constructs have been described previously (19). HEK293T or HeLa cells were transfected for 24 h with the appropriate constructs using Lipofectamine 2000 (Invitrogen) in accordance with the manufacturer's instructions. Cells were lysed in radioimmunoprecipitation assay buffer. Clarified lysates were incubated with anti-V5 or anti-FLAG antibody-conjugated agarose beads for 2 h at 4 °C. For Western blotting, beads were washed in phosphate-buffered saline, reconstituted in NuPAGE sample loading buffer (containing 30% (v/v) NuPAGE reducing agent; Invitrogen), and heated at 80 °C for 10 min to elute immunopurified proteins.

Mass Spectrometry—Following anti-V5 immunopurification of clarified cell lysates, bead-bound Keap1-V5/His was washed in phosphate buffer (67.3 mM Na_2HPO_4, 13.1 mM KH_2PO_4, pH 7.4) and incubated with 1 mM dithiothreitol for 15 min. Following several more washes, Keap1-V5/His was incubated with 20 mM *N*-ethylmaleimide for 15 min. All incubations were at 4 °C. Keap1-V5/His was digested with 400 ng of trypsin (Promega) overnight at 37 °C, and the resulting peptides were analyzed by LC-ESI-MS/MS. Samples were delivered into an API QSTAR Pulsar i system (Applied Biosystems) by automated in-line chromatography, using an integrated LCPackings System and 75-μm × 15-cm C18 PepMap column (Dionex, Camberley, UK), via a nanoelectrospray source head and 10-μm inner diameter PicoTip (New Objective, Woburn, MA). The LC conditions were: 5% (v/v) acetonitrile, 0.05% (v/v) trifluoroacetic acid for 15 min, 5–48% acetonitrile, 0.05% trifluoroacetic acid over 60 min, 99% acetonitrile, 0.05% trifluoroacetic acid for 10 min, 5% acetonitrile, 0.05% trifluoroacetic acid for 10 min, with a flow rate of 0.35 μl/min throughout. MS and MS/MS spectra were acquired automatically in positive ion mode using information-dependent acquisition powered by Analyst QS software (Applied Biosystems). The three most intense ions in each MS spectrum were subjected to MS/MS analysis for 2 s and subsequently excluded from further analysis for 40 s. Proteins present in the immunopurified fraction were identified with ProteinPilot software version 3.0 (Applied Biosystems) using the Paragon™ algorithm (20) and the most recent version of the SwissProt data base. Protein identifications were accepted if they fell within the 5% local false discovery rate, determined by searching against the reversed SwissProt data base, and if at least two peptides were identified with a confidence >95%. The mass accuracy of each peptide ion was determined at 5–30 ppm.

Immunoprecipitation—Endogenous SQSTM1 was immunoprecipitated from HEK293T cells, which were lysed in radioimmunoprecipitation assay buffer. The lysate was precleared by incubation with protein A-Sepharose 4B for 1 h at 4 °C. The precleared lysate was then divided equally and incubated for 2 h with or without 2 μg of a rabbit anti-human SQSTM1 antibody (Sigma-Aldrich). The lysates were then supplemented with protein A-Sepharose 4B and incubated for a further 1 h. The beads were washed in radioimmunoprecipitation assay buffer followed by phosphate-buffered saline, reconstituted in NuPAGE sample loading buffer, and heated at 80 °C for 10 min to elute immunoprecipitated proteins.

RNA Interference—Short interfering RNA (siRNA) duplexes targeted against human SQSTM1 (D-010230-03, subsequently referred to as si-SQSTM1 h3), mouse SQSTM1 (D-047628-03 and D-047628-04, subsequently referred to as si-SQSTM1 m3 and m4, respectively), and a scrambled nontargeting control siRNA duplex (D-001210-03, subsequently referred to as si-CON), were purchased from the Dharmacon (Lafayette, CO) siGENOME library. Cells were transfected with 10 nM siRNA using Lipofectamine RNAiMAX (Invitrogen) in accordance with the manufacturer's instructions.

Immunocytochemistry and Confocal Microscopy—Hepa-1c1c7 cells were seeded onto Lab-TEK II chamber slides (Nalge Nunc, Rochester, NY) and transfected with siRNA for 48 h. Cells were fixed in 4% paraformaldehyde at 4 °C for 30 min. Fixed cells were permeabilized with 0.2% Triton X-100, quenched with 100 mM glycine, and blocked with 10% fetal bovine serum, for 10 min each. Cells were then incubated with an anti-SQSTM1 antibody (1:500) in 2% fetal bovine serum at 37 °C for 1 h. Following repeated washes in phosphate-buffered saline, cells were incubated with an anti-rabbit IgG fluorescein isothiocyanate conjugate (Sigma-Aldrich) in 2% fetal bovine serum at 37 °C for 1 h. Cells were then washed repeatedly, and nuclei were counterstained with Hoechst 33258 (2 μg/ml; Invitrogen) in phosphate-buffered saline at room temperature for 10 min. Immunofluorescence was visualized using a Leica SP2 AOBS confocal microscope (Leica Microsystems, Milton Keynes, UK). Multiple fields were evaluated for each condition (representative fields are presented).

Western Blot Analysis—Cells were transfected with expression constructs for 48 h or siRNA for 48 or 72 h, and lysates were prepared and analyzed by Western blotting as described previously (11). SQSTM1 was probed with a rabbit anti-human SQSTM1 antibody for 1 h at 1:10,000 in Tris-buffered saline-Tween containing 2% nonfat dry milk (Bio-Rad Laboratories). Immunoreactive band volumes were quantified using TotalLab

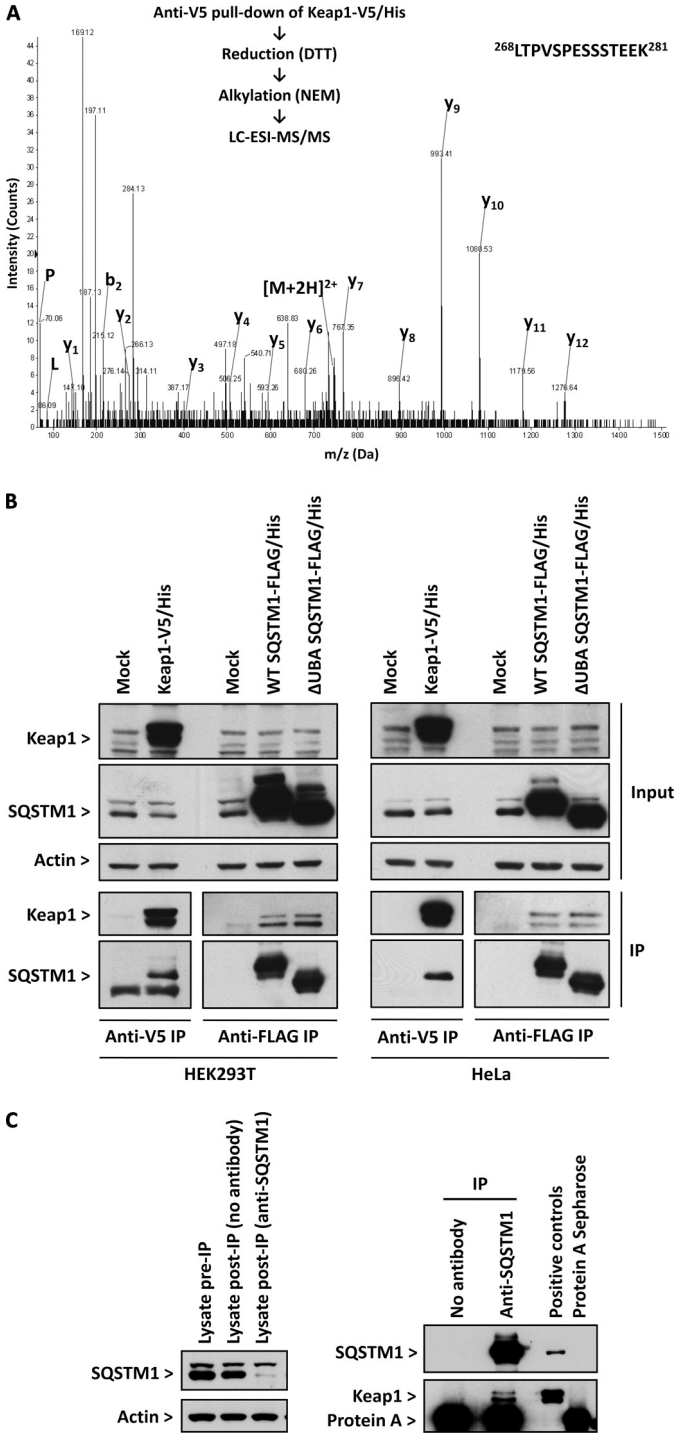

FIGURE 1. **SQSTM1 associates with Keap1 in mammalian cells.** *A*, overview of proteomic approach used to identify SQSTM1 as a binding partner of Keap1. HEK293T cells were transfected with Keap1-V5/His, which was purified, by anti-V5 pulldown, from cell lysates, reduced, alkylated, and digested overnight with trypsin. The resulting tryptic peptides were analyzed by LC-ESI-MS/MS. Proteins present in the immunopurified fraction were identified via reference to the expected masses of their tryptic peptides. The MS/MS spectrum depicts the SQSTM1 peptide ^{268}LTPVSPESSSTEEK^{281}, $[M+2H]^{2+}$ = 745.9 atomic mass units. y- and b-ions are labeled where present. Immonium ions are labeled with the one-letter code for their corresponding amino acid. *DTT*, dithiothreitol; *NEM*, *N*-ethylmaleimide. *B*, Keap1-V5/His or SQSTM1-FLAG/His were ectopically expressed in HEK293T or HeLa cells. Lysates were prepared and incubated with anti-V5 or anti-FLAG antibody-conjugated agarose beads, and immunopurified Keap1 and SQSTM1 were analyzed by Western blotting. *Input* represents 5% of the total cell material preimmunopurification. β-Actin was probed as a loading control. *C*, HEK293T cells were lysed and subjected to immunoprecipitation (*IP*) with an anti-SQSTM1 antibody and protein A-conjugated beads. A similar procedure was performed without the anti-SQSTM1 antibody as a control. Lysates and immunoprecipitated proteins were analyzed by Western blotting. Lysates before and after immunoprecipitation represent 5% of the total cell material. Lysates from HEK293T cells in which SQSTM1 and Keap1 had been ectopically expressed were loaded as positive controls. The inherent immunoreactivity of protein A-Sepharose was also determined as a control.

100 software (Nonlinear Dynamics, Newcastle, UK) and normalized to β-actin, which was probed as a loading control.

Real-time RT-PCR Quantification of mRNA—Hepa-1c1c7 cells were transfected with siRNA for 48 h, and total RNA was isolated using TRIzol reagent (Invitrogen), in accordance with the manufacturer's instructions. cDNA was synthesized using the ImProm-II reverse transcription system (Promega). The levels of Nrf2, Keap1, heme oxygenase 1, glutamate-cysteine ligase catalytic subunit (GCLC) and NAD(P)H:quinone oxidoreductase 1 gene expression were determined using 50 ng of cDNA and SYBR Green JumpStart Taq Ready Mix, using GAPDH as an internal standard for normalization. Gene-specific primers (supplemental Table 1) were synthesized by Sigma-Aldrich. Quantitative real-time PCR was performed on an ABI PRISM 7000 Sequence Detection system (Applied Biosystems). Samples prepared without reverse transcriptase, which produced negligible signals, served as negative controls.

Measurement of Glutathione—Hepa-1c1c7 cells were transfected with siRNA for 72 h, and total cellular glutathione (GSH) content was quantified as previously described (11).

Data Analysis—Data are expressed as mean ± S.D. of the mean from at least three independent experiments. The significance of differences within the data were assessed by one-way analysis of variance (with Tukey's post test) or Kruskal-Wallis (with Conover-Inman post test). A two-sided p value of ≤0.05 was considered to be statistically significant.

RESULTS

SQSTM1 Interacts with Keap1—Previously, we used LC-ESI-MS/MS to identify the cysteine residues in mouse Keap1-V5/His that are selectively modified by a panel of Nrf2-activating molecules in HEK293T cells (11). During the course of this investigation, we noted that the multifunctional protein SQSTM1 was consistently identified as being present in the pulldown fraction alongside Keap1-V5/His (Fig. 1*A* and supplemental Tables 2 and 3). This raised the possibility that SQSTM1 was a binding partner of Keap1.

To confirm the association of Keap1 with SQSTM1, we expressed human Keap1-V5/His or SQSTM1-FLAG/His in HEK293T or HeLa cells and subjected cell lysates to anti-V5 or anti-FLAG pulldown followed by immunoblotting for Keap1 or SQSTM1. In both cell lines, endogenous SQSTM1 was only present in the anti-V5 pulldowns when Keap1-V5/His was expressed in cells (Fig. 1*B*). In the reverse experiment, endogenous Keap1 was only present in the anti-FLAG pulldowns when SQSTM1-FLAG/His was expressed in cells (Fig. 1*B*). Importantly, a ΔUBA SQSTM1-FLAG/His mutant lacking the ubiquitin-associated domain was also capable of binding endogenous Keap1 in HEK293T and HeLa cells (Fig. 1*B*), demonstrating that the interaction between Keap1 and

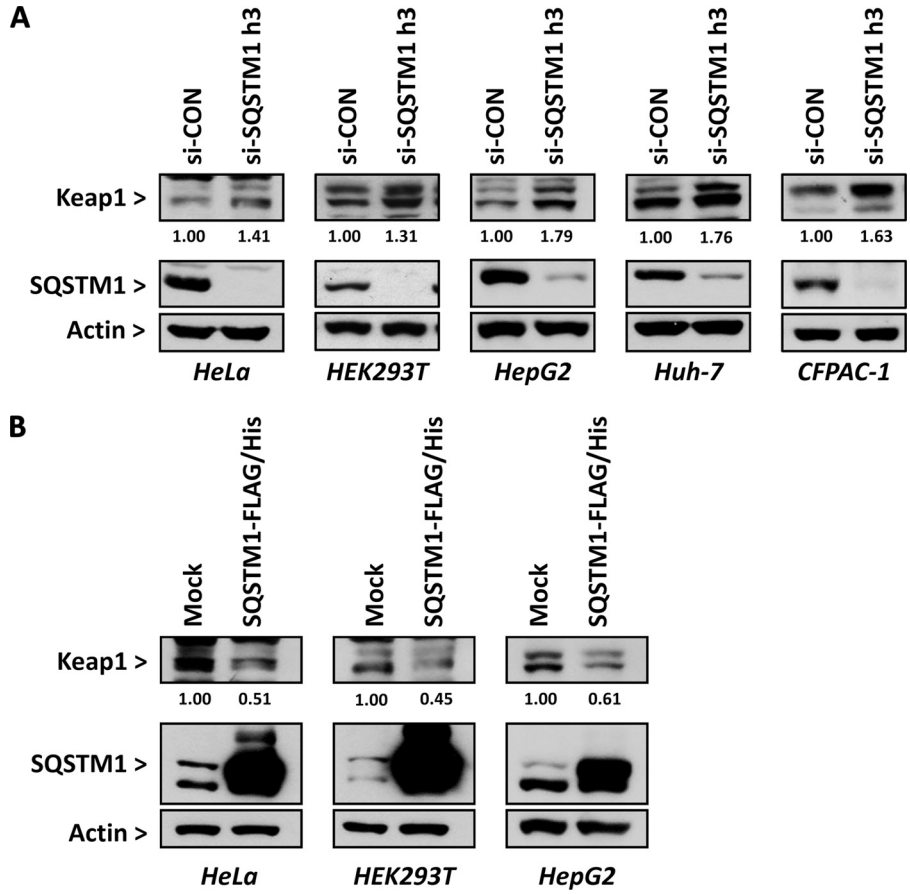

FIGURE 2. **Manipulation of SQSTM1 levels affects the basal protein level of Keap1 in a panel of human cell lines.** *A*, HeLa, HEK293T, HepG2, Huh-7 and CFPAC-1 cells were transfected with a scrambled control siRNA (si-CON) or SQSTM1-targeting siRNA (si-SQSTM1 h3) for 48 h. Keap1 and SQSTM1 levels were analyzed by Western blotting. Immunoreactive band volumes were quantified by densitometry and expressed relative to β-actin to enable comparison of Keap1 protein levels in cells transfected with si-CON, which were arbitrarily set at 1.00, and those transfected with si-SQSTM1 h3. Relative Keap1 levels are presented beneath the Keap1 blot. *B*, HeLa, HEK293T, and HepG2 cells were mock transfected or transfected with a SQSTM1-FLAG/His construct for 48 h. Keap1 and SQSTM1 levels were analyzed by Western blotting. Immunoreactive band volumes were quantified by densitometry and expressed relative to β-actin to enable comparison of Keap1 protein levels in mock transfected cells, which were arbitrarily set at 1.00, and those transfected with SQSTM1-FLAG/His. Relative Keap1 levels are presented beneath the Keap1 blot.

SQSTM1 was not dependent on the presence of the ubiquitin-associated domain of SQSTM1 and implying that the ubiquitination of Keap1 is not required for its association with SQSTM1.

To verify that Keap1 and SQSTM1 interact under physiological conditions, endogenous SQSTM1 was immunoprecipitated from HEK293T cells. Endogenous Keap1 was identified as a co-precipitating protein (Fig. 1*C*), demonstrating that SQSTM1 is a binding partner of Keap1 under physiological conditions.

SQSTM1 Influences the Basal Integrity of the Keap1-Nrf2 Pathway by Regulating the Degradation of Keap1—To investigate the biological significance of the interaction between Keap1 and SQSTM1, we examined the effect on Keap1 of depleting endogenous SQSTM1, using siRNA, or ectopically expressing SQSTM1-FLAG/His in a panel of human cell lines originating from discrete organs. In HeLa (cervical adenocarcinoma), HEK293T (kidney), HepG2 (hepatocellular carcinoma), Huh-7 (hepatocellular carcinoma), and CFPAC-1 (pancreatic ductal adenocarcinoma) cells, depletion of SQSTM1 with si-SQSTM1 h3 consistently resulted in a increase in the basal protein level of Keap1 (Fig. 2*A*). Conversely, ectopic expression of SQSTM1-FLAG/His in HeLa, HEK293T, and HepG2 cells consistently caused a decrease in the basal protein level of Keap1 (Fig. 2*B*). We were unable to express SQSTM1-FLAG/His in Huh-7 or CFPAC-1 cells.

To explore further the biological consequences of siRNA depletion of SQSTM1 on the Keap1-Nrf2 pathway, mouse Hepa-1c1c7 cells were transfected with si-SQSTM1 m3 (Fig. 3*A*) or m4. In these cells, si-SQSTM1 m3 and m4 caused a 7.2- and 9.2-fold increase, respectively, in the basal protein level of Keap1 (Fig. 3*B*). Concurrently, depletion of SQSTM1 with si-SQSTM1 m3 and m4 resulted in an 89 and 71% decrease, respectively, in the basal protein level of Nrf2 (Fig. 3*B*). The changes in basal Keap1 and Nrf2 protein levels were not due to the altered transcription of the respective genes because siRNA depletion of SQSTM1 did not significantly affect the mRNA levels of Keap1 or Nrf2 in Hepa-1c1c7 cells (Fig. 3*C*). These results indicate that SQSTM1 regulates the integrity of the Keap1-Nrf2 pathway in a posttranscriptional manner.

To explore the biochemical mechanisms underpinning the changes in Keap1 and Nrf2 protein levels upon manipulation of SQSTM1, Hepa-1c1c7 cells were transfected with si-CON or si-SQSTM1 m3 and then exposed to the protein synthesis inhibitor cycloheximide for up to 16 h. In si-CON-transfected cells, the half-life of Keap1 was 11.3 h (Fig. 3*D*). In si-SQSTM1-transfected cells, however, the half-life of Keap1 almost doubled to 21.1 h (Fig. 3*D*), indicating that siRNA depletion of SQSTM1 causes an increase in the basal protein level of Keap1 by slowing its rate of degradation. Notably, the reduction in the basal level of Nrf2 upon siRNA depletion of SQSTM1 did not compromise the inducibility of the Keap1-Nrf2 pathway, as demonstrated by the marked accumulation of Nrf2 in both si-CON and si-SQSTM1 m3-transfected Hepa-1c1c7 cells exposed to iodoacetamide or *tert*-butylhydroquinone for 1 h (Fig. 3*E*). These results indicate that SQSTM1 can influence the basal level of Keap1 by regulating its degradation and therefore contribute to the integrity of the Keap1-Nrf2 pathway. However, SQSTM1 appears to be dispensable for the induction of Nrf2.

SQSTM1 Contributes to the Basal Cell Defense Capacity—Given that siRNA depletion of SQSTM1 resulted in a decrease

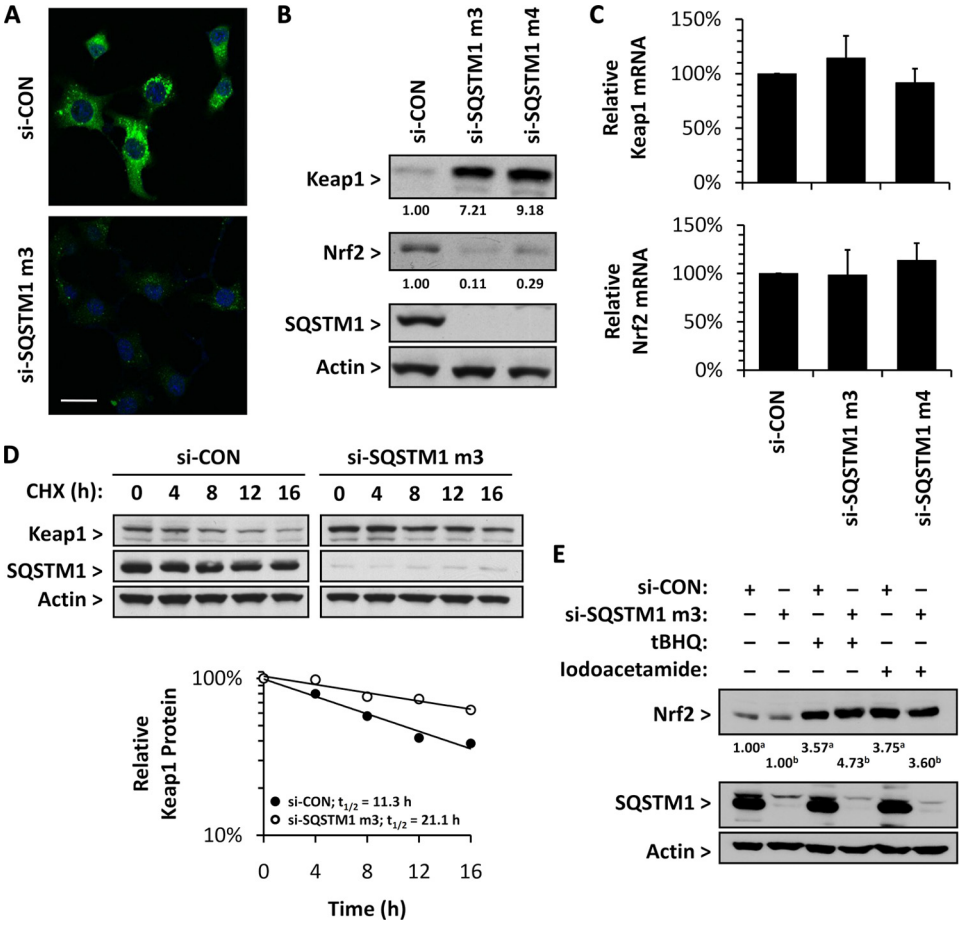

FIGURE 3. **Depletion of SQSTM1 affects the basal protein levels of Keap1 and Nrf2, through a decrease in the rate of degradation of Keap1, but does not compromise the inducibility of Nrf2.** Hepa-1c1c7 cells were transfected with a scrambled control siRNA (si-CON) or SQSTM1-targetting siRNA (si-SQSTM1 m3 or m4) for 48 h. *A*, immunocytochemical analysis of total cellular SQSTM1 (*green*) levels following transfection with si-CON or si-SQSTM1 m3, as visualized by confocal microscopy. Nuclei were counterstained with Hoechst 33258 (*blue*). Each image represents an overlay of SQSTM1 and Hoechst signals. *Scale bar*, 50 μm. *B*, Western blot analysis of Keap1, Nrf2, and SQSTM1 in siRNA-transfected cells. Immunoreactive band volumes were quantified by densitometry and expressed relative to β-actin to enable comparison of Keap1 and Nrf2 protein levels in cells transfected with si-CON, which were arbitrarily set at 1.00, and those transfected with si-SQSTM1 m3 or m4. Relative Keap1 and Nrf2 levels are presented beneath the respective blots. *C*, relative levels of Keap1 and Nrf2 mRNA in siRNA-transfected cells, as determined by real-time RT-PCR using SYBR Green and gene-specific primers. Keap1 and Nrf2 mRNA levels were normalized to GAPDH mRNA levels in the same samples. The mRNA levels in si-SQSTM1-transfected cells are expressed relative to those detected in si-CON-transfected cells. *D*, siRNA-transfected cells exposed to cycloheximide (*CHX*; 35 μM) for the indicated times. Keap1 and SQSTM1 levels were analyzed by Western blotting. Immunoreactive band volumes were quantified by densitometry and expressed relative to β-actin to enable comparison of the Keap1 protein level at 0 h, which was arbitrarily set at 1.00, with that at subsequent time points. Relative levels of Keap1 are presented in the *scatterplot*. *E*, Western blot analysis of Nrf2 and SQSTM1 following exposure of siRNA-transfected cells to the Nrf2-activators *tert*-butylhydroquinone (*tBHQ*) or iodoacetamide (both 50 μM) for 1 h. Immunoreactive band volumes were quantified by densitometry and expressed relative to β-actin to enable comparison of Nrf2 protein levels in vehicle-exposed cells transfected with si-CON^a or si-SQSTM1 m3^b, which were arbitrarily set at 1.00, and those exposed to *tert*-butylhydroquinone or iodoacetamide. Relative Nrf2 levels are presented beneath the Nrf2 blot.

in the basal protein level of Nrf2, we hypothesized that this would correspond to a decrease in the capacity of Nrf2-regulated cell defense processes. In Hepa-1c1c7 cells transfected with si-SQSTM1 m3 and m4, the basal mRNA level of three Nrf2-regulated genes, heme oxygenase 1, GCLC, and NAD(P)H:quinone oxidoreductase 1, was reduced significantly, between 37 and 61% compared with si-CON-transfected cells (Fig. 4*A*). Furthermore, the basal protein level of GCLC was decreased by 39 and 41% in cells transfected with si-SQSTM1 m3 and m4, respectively (Fig. 4*B*). In keeping with its role as the rate-limiting enzyme in the synthesis of GSH, the functional significance of the decrease in basal mRNA and protein level of GCLC through depletion of SQSTM1 was demonstrated by the 17 and 16% decrease in the basal level of GSH in cells transfected with si-SQSTM1 m3 and m4, respectively (Fig. 4*C*). These results further indicate that SQSTM1 regulates the basal activity of the Keap1-Nrf2 pathway and thus contributes to the capacity of a cell to defend itself against chemical/oxidative stress.

DISCUSSION

In this study, we have shown that SQSTM1, whose major functions include (i) serving as a scaffold in various signaling pathways through its multiple protein-protein interaction motifs, (ii) sequestering damaged and misfolded proteins into aggregates prior to their degradation, and (iii) shuttling polyubiquitinated proteins to the proteasomal and lysosomal degradation machineries (18), interacts both physically and functionally with Keap1, the negative regulator of the cytoprotective transcription factor Nrf2. In doing so, we have provided evidence that SQSTM1 can control the integrity of the Keap1-Nrf2 pathway, by regulating the degradation of Keap1 and, consequently, the basal activity of Nrf2. To our knowledge, this provides the first evidence for a post-translational mechanism regulating the basal activity of Keap1.

In addition to Nrf2, Keap1 has been reported to associate with several other proteins in mammalian cells. For example, Keap1 associates with PGAM5, which reportedly tethers Keap1 and Nrf2 to the outer membrane of the mitochondria (16, 17), implying that the Keap1·Nrf2 complex may be well placed to sense the disruption of mitochondrial function and subsequent elevated generation of reactive oxygen species that can contribute to the onset of oxidative stress. In a confirmation of previous reports (16, 17), we noted that PGAM5 was consistently identified as a Keap1-interacting protein in our LC-ESI-MS/MS study (supplemental Table 4).

IκB kinase β (IKKβ) has also been described as a binding partner of Keap1 in cells (21). IKKβ regulates the activity of the transcription factor nuclear factor κB (NF-κB) by phosphory-

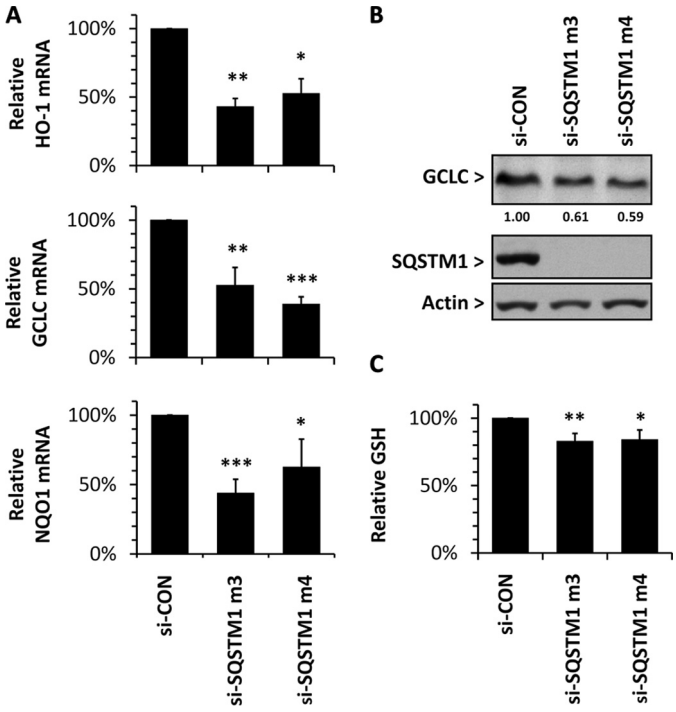

FIGURE 4. **Depletion of SQSTM1 causes a decrease in basal mRNA level, protein level, and function of several Nrf2-regulated cell defense genes.** Hepa-1c1c7 cells were transfected with a scrambled control siRNA (si-CON) or SQSTM1-targeting siRNA (si-SQSTM1 m3 or m4) for 48 h (*A*) or 72 h (*B* and *C*). *A*, relative levels of heme oxygenase 1 (*HO-1*), GCLC, and NAD(P)H:quinone oxidoreductase 1 (*NQO1*) mRNA, as determined by real-time RT-PCR using SYBR Green and gene-specific primers. Heme oxygenase 1, GCLC, and NAD(P)H:quinone oxidoreductase 1 mRNA levels were normalized to GAPDH mRNA levels in the same samples. The mRNA levels in si-SQSTM1-transfected cells are expressed relative to those detected in si-CON-transfected cells. *, $p \leq 0.05$; **, $p \leq 0.01$; ***, $p \leq 0.001$ *versus* si-CON (Kruskal-Wallis). *B*, Western blot analysis of GCLC and SQSTM1. Immunoreactive band volumes were quantified by densitometry and expressed relative to β-actin to enable comparison of GCLC protein level in cells transfected with si-CON, which was arbitrarily set at 1.00, and those transfected with si-SQSTM1 m3 or m4. Relative GCLC levels are presented beneath the GCLC blot. *C*, relative levels of total GSH, normalized to total protein content. The GSH levels in si-SQSTM1-transfected cells are expressed relative to those measured in si-CON-transfected cells. *, $p \leq 0.05$; **, $p \leq 0.01$ *versus* si-CON (one-way analysis of variance).

lating, and consequently inactivating, the cytosolic inhibitors of κB (21). Keap1 was shown to be responsible for the ubiquitination, and subsequent degradation, of IKKβ, so that induction of Keap1 results in a decrease in the activity of the NF-κB pathway, through the enhanced turnover of IKKβ (21). Depletion of SQSTM1 is known to cause a decrease in NF-κB activity (22), and we have shown here that depletion of SQSTM1 is associated with an induction of Keap1 and repression of Nrf2. Taken together, these findings suggest that SQSTM1 serves as a regulatory node in several signaling cascades that contribute to the maintenance of cellular homeostasis.

In a very recent report (23), Komatsu and colleagues have demonstrated an interaction between Keap1 and SQSTM1 and have defined the motifs in Keap1 and SQSTM1 responsible for this interaction. SQSTM1 binds to the bottom side of the six-bladed β-propeller structure formed by the DC (double glycine repeat and C-terminal) domain of Keap1 (23). As with Nrf2 (8), PGAM5 (16, 17) and IKKβ (21), the Keap1-interacting motif in SQSTM1 conforms to the consensus sequence (D/N)*X*(E/S)(T/S)GE (23). Notably, the Keap1-interacting motif identified by Komatsu *et al.* (23) lies outside of the ubiquitin-associated domain of SQSTM1, consistent with our finding that this domain is dispensable for the interaction with Keap1. In agreement wih Liu *et al.* (24), who observed an induction of Nrf2-dependent cell defence processes following ectopic expression of SQSTM1 in IMR-32 human neuroblastoma cells, Komatsu and colleagues demonstrated that overproduction of SQSTM1 was shown to cause an increase in the cellular Nrf2 level by competing with Nrf2 for binding to Keap1, disrupting the ability of the latter to direct the ubiquitination of Nrf2 efficiently (23). However, we have demonstrated that the ability of SQSTM1 to regulate the basal protein level of Nrf2 is also due to its capacity to alter the basal protein level of Keap1, by affecting its rate of degradation. In light of the observation of Komatsu and colleagues that ectopic expression of SQSTM1 causes a decrease in the ubiquitination of Nrf2, and in turn an increase in the total cellular level of the transcription factor (23), it is plausible that the decrease in total cellular level of Nrf2 following siRNA depletion of SQSTM1 reported here is due to an increase in Keap1-directed ubiquitination of Nrf2, facilitated by the higher basal level of Keap1.

Together with the proteasome, autophagy (literally "self-eating") is responsible for the majority of cellular protein degradation. Following sequestration within autophagic vacuoles, organelles and cytoplasmic fractions are delivered to lysosomes for degradation (25). SQSTM1 targets proteins for degradation via autophagy by associating with ubiquitin on the substrate and with components of the autophagy machinery, including Atg8/LC3 (26). The basal protein level of Keap1 has been shown to be raised in autophagy-deficient cells (23), implying that Keap1 is at least partly degraded via autophagy. It is important to note that SQSTM1 expression is itself up-regulated in an Nrf2-dependent manner under conditions of chemical/oxidative stress (27, 28), and it is therefore possible that SQSTM1 forms part of a regulatory feedback loop in the Keap1-Nrf2 pathway. Under conditions of Nrf2 activation, the elevated expression of SQSTM1 may enable the targeting of Keap1 for degradation via autophagy, which in turn may (i) further contribute to the activation of Nrf2 and/or (ii) represent a means by which modified/inactivated Keap1 is removed/recycled to restore homeostasis in the pathway (Fig. 5). The regulation of the Keap1-Nrf2 pathway by autophagy warrants further exploration.

More than 20 different mutations in the SQSTM1 gene have been identified in patients diagnosed with Paget's disease of bone, a common disorder of bone-resorbing osteoclasts that causes increased bone turnover and is associated with several complications including bone pain, osteoarthritis, and pathological fracture (29). The overwhelming majority of these mutations result in an impaired ability of SQSTM1 to bind ubiquitin (29). SQSTM1 is an important component of a signaling pathway that regulates the activity of NF-κB, which partly controls osteoclastogenesis and the bone-resorbing activity of mature osteoclasts, and it appears that dysfunction of SQSTM1 induces NF-κB-dependent cellular processes, causing increased osteoclast-mediated bone turnover (29). In light of our finding that SQSTM1 can regulate the activity of the Keap1-

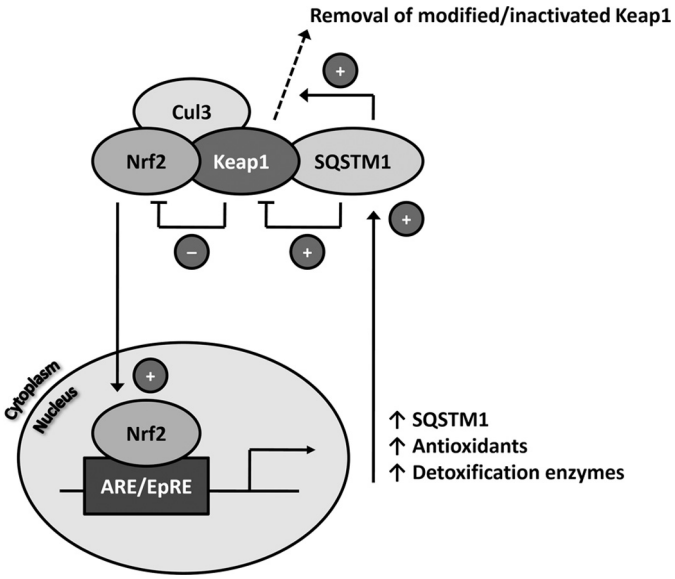

FIGURE 5. **Model for the role of SQSTM1 in regulating the integrity of the Keap1-Nrf2 cell defense pathway.** This study has demonstrated that SQSTM1 associates with Keap1 in cells and contributes to the integrity of the Keap1-Nrf2 pathway by regulating the basal levels of Keap1 and Nrf2. Recent work has demonstrated increased levels of Keap1 in autophagy-deficient cells (23). SQSTM1 expression is itself up-regulated in an Nrf2-dependent manner under conditions of chemical/oxidative stress (27, 28), suggesting that SQSTM1 forms part of a regulatory feedback loop in the Keap1-Nrf2 pathway. Under conditions of Nrf2 activation, the elevated expression of SQSTM1 may enable the targeting of Keap1 for degradation via autophagy, which in turn may (i) further contribute to the activation of Nrf2 and/or (ii) represent a means by which modified/inactivated Keap1 is removed/recycled to restore homeostasis in the pathway. *ARE/EpRE*, antioxidant response element/electrophile response element.

Nrf2 cytoprotective pathway, it will be important to determine the role of Nrf2 in the molecular pathogenesis of Paget's disease of bone.

In summary, this study has presented evidence for a physical and functional interaction between Keap1 and SQSTM1 in mammalian cells. In demonstrating that SQSTM1 regulates the degradation of Keap1, this work has uncovered an additional layer of regulatory control within the Keap1-Nrf2 cytoprotective pathway.

Acknowledgments—We thank Drs. Caroline Earnshaw and Victoria Elliot for help with mass spectrometry, Dr. Alec Simpson for assistance with confocal microscopy, and Dr. Laura Randle for help with real-time RT-PCR. The confocal microscopy work was carried out in the Department of Human Anatomy and Cell Biology, School of Biomedical Sciences, the University of Liverpool, United Kingdom.

REFERENCES

1. Copple, I. M., Goldring, C. E., Kitteringham, N. R., and Park, B. K. (2008) *Toxicology* **246,** 24–33
2. Chan, K., Han, X. D., and Kan, Y. W. (2001) *Proc. Natl. Acad. Sci. U.S.A.* **98,** 4611–4616
3. Rangasamy, T., Cho, C. Y., Thimmulappa, R. K., Zhen, L., Srisuma, S. S., Kensler, T. W., Yamamoto, M., Petrache, I., Tuder, R. M., and Biswal, S. (2004) *J. Clin. Invest.* **114,** 1248–1259
4. Ramos-Gomez, M., Kwak, M. K., Dolan, P. M., Itoh, K., Yamamoto, M., Talalay, P., and Kensler, T. W. (2001) *Proc. Natl. Acad. Sci. U.S.A.* **98,** 3410–3415
5. Cullinan, S. B., Gordan, J. D., Jin, J., Harper, J. W., and Diehl, J. A. (2004) *Mol. Cell. Biol.* **24,** 8477–8486
6. Kobayashi, A., Kang, M. I., Okawa, H., Ohtsuji, M., Zenke, Y., Chiba, T., Igarashi, K., and Yamamoto, M. (2004) *Mol. Cell. Biol.* **24,** 7130–7139
7. Zhang, D. D., Lo, S. C., Cross, J. V., Templeton, D. J., and Hannink, M. (2004) *Mol. Cell. Biol.* **24,** 10941–10953
8. Tong, K. I., Kobayashi, A., Katsuoka, F., and Yamamoto, M. (2006) *Biol. Chem.* **387,** 1311–1320
9. Dinkova-Kostova, A. T., Holtzclaw, W. D., Cole, R. N., Itoh, K., Wakabayashi, N., Katoh, Y., Yamamoto, M., and Talalay, P. (2002) *Proc. Natl. Acad. Sci. U.S.A.* **99,** 11908–11913
10. Hong, F., Sekhar, K. R., Freeman, M. L., and Liebler, D. C. (2005) *J. Biol. Chem.* **280,** 31768–31775
11. Copple, I. M., Goldring, C. E., Jenkins, R. E., Chia, A. J., Randle, L. E., Hayes, J. D., Kitteringham, N. R., and Park, B. K. (2008) *Hepatology* **48,** 1292–1301
12. Sekhar, K. R., Rachakonda, G., and Freeman, M. L. (2010) *Toxicol. Appl. Pharmacol.* **244,** 21–26
13. Kang, M. I., Kobayashi, A., Wakabayashi, N., Kim, S. G., and Yamamoto, M. (2004) *Proc. Natl. Acad. Sci. U.S.A.* **101,** 2046–2051
14. Furukawa, M., and Xiong, Y. (2005) *Mol. Cell. Biol.* **25,** 162–171
15. Karapetian, R. N., Evstafieva, A. G., Abaeva, I. S., Chichkova, N. V., Filonov, G. S., Rubtsov, Y. P., Sukhacheva, E. A., Melnikov, S. V., Schneider, U., Wanker, E. E., and Vartapetian, A. B. (2005) *Mol. Cell. Biol.* **25,** 1089–1099
16. Lo, S. C., and Hannink, M. (2006) *J. Biol. Chem.* **281,** 37893–37903
17. Lo, S. C., and Hannink, M. (2008) *Exp. Cell Res.* **314,** 1789–1803
18. Seibenhener, M. L., Geetha, T., and Wooten, M. W. (2007) *FEBS Lett.* **581,** 175–179
19. Najat, D., Garner, T., Hagen, T., Shaw, B., Sheppard, P. W., Falchetti, A., Marini, F., Brandi, M. L., Long, J. E., Cavey, J. R., Searle, M. S., and Layfield, R. (2009) *J. Bone Miner. Res.* **24,** 632–642
20. Shilov, I. V., Seymour, S. L., Patel, A. A., Loboda, A., Tang, W. H., Keating, S. P., Hunter, C. L., Nuwaysir, L. M., and Schaeffer, D. A. (2007) *Mol. Cell. Proteomics* **6,** 1638–1655
21. Lee, D. F., Kuo, H. P., Liu, M., Chou, C. K., Xia, W., Du, Y., Shen, J., Chen, C. T., Huo, L., Hsu, M. C., Li, C. W., Ding, Q., Liao, T. L., Lai, C. C., Lin, A. C., Chang, Y. H., Tsai, S. F., Li, L. Y., and Hung, M. C. (2009) *Mol. Cell* **36,** 131–140
22. Moscat, J., and Diaz-Meco, M. T. (2009) *Cell* **137,** 1001–1004
23. Komatsu, M., Kurokawa, H., Waguri, S., Taguchi, K., Kobayashi, A., Ichimura, Y., Sou, Y. S., Ueno, I., Sakamoto, A., Tong, K. I., Kim, M., Nishito, Y., Iemura, S., Natsume, T., Ueno, T., Kominami, E., Motohashi, H., Tanaka, K., and Yamamoto, M. (2010) *Nat. Cell Biol.* **12,** 213–223
24. Liu, Y., Kern, J. T., Walker, J. R., Johnson, J. A., Schultz, P. G., and Luesch, H. (2007) *Proc. Natl. Acad. Sci. U.S.A.* **104,** 5205–5210
25. Maiuri, M. C., Zalckvar, E., Kimchi, A., and Kroemer, G. (2007) *Nat. Rev. Mol. Cell Biol.* **8,** 741–752
26. Pankiv, S., Clausen, T. H., Lamark, T., Brech, A., Bruun, J. A., Outzen, H., Øvervatn, A., Bjørkøy, G., and Johansen, T. (2007) *J. Biol. Chem.* **282,** 24131–24145
27. Ishii, T., Itoh, K., Takahashi, S., Sato, H., Yanagawa, T., Katoh, Y., Bannai, S., and Yamamoto, M. (2000) *J. Biol. Chem.* **275,** 16023–16029
28. Warabi, E., Takabe, W., Minami, T., Inoue, K., Itoh, K., Yamamoto, M., Ishii, T., Kodama, T., and Noguchi, N. (2007) *Free Radic. Biol. Med.* **42,** 260–269
29. Layfield, R., and Searle, M. S. (2008) *Biochem. Soc. Trans.* **36,** 469–471